Draft version December 6, 2006
Preprint typeset using LaTeX style emulateapj v. 10/09/06

GEMINI SPECTROSCOPIC SURVEY OF YOUNG STAR CLUSTERS IN MERGING/INTERACTING GALAXIES. I. NGC 3256 TIDAL-TAIL CLUSTERS

Gelys Trancho
Universidad de La Laguna, Tenerife, Canary Island, Spain and
Gemini Observatory, 670 N. A'ohoku Place, Hilo, HI 96720, USA

Nate Bastian
Department of Physics and Astronomy, University College London, Gower Street, London, WC1E 6BT, United Kingdom

François Schweizer
Carnegie Observatories, 813 Santa Barbara Street, Pasadena CA 91101-1292, USA

and

Bryan W. Miller
Gemini Observatory, Casilla 603, La Serena, Chile

Draft version December 6, 2006

ABSTRACT

We present Gemini optical spectroscopy of three young star clusters in the western tidal tail of NGC 3256. Compact star clusters (as opposed to dwarf-galaxy candidates) in tidal tails are rare, with these three clusters the first for which detailed quantitative spectroscopy has ever been obtained. We find that two of these clusters appear to be coeval, while the third is approximately two times older (∼200 Myr vs. ∼80 Myr). All three clusters are massive ($1–3 \times 10^5 \mathcal{M}_\odot$) and appear to be of roughly solar metallicity. Additionally, the three clusters appear to be relatively large ($R_{eff} = 10 - 20$ pc), possibly reflecting weak compression at the time of formation and/or the weak influence of the tidal field of the galaxy. All three clusters have velocities consistent with the general trend of the H I velocities in the tidal tail. We conclude that if the loosely bound tail material of NGC 3256 gets stripped during future interactions of this galaxy within its group, these three clusters may become part of the intra-group medium.

Subject headings: globular clusters: general — globular clusters: individual(NGC 3256

1. INTRODUCTION

Massive star clusters are usually considered to be components of galaxies, however there is a growing body of evidence that there are also populations of star clusters that may be bound to the gravitational potential of galaxy groups and clusters rather than to individual galaxies (West et al. 1995; Kissler-Patig et al. 1999; Bassino et al. 2003; Jordán et al. 2003). As with the intracluster stars (Ferguson et al. 1998; Mihos et al. 2005; Krick et al. 2005) and PNe (Aguerri et al. 2005) it is thought that these star clusters are mostly old objects stripped from galaxies as they interact with other galaxies in their group or cluster (Murante et al. 2004; Yahagi & Bekki 2005). Alternatively, *young* star clusters formed during galaxy mergers and interactions may also get flung into the intracluster environment. This paper investigates the plausiblility of this process using spectroscopy of young star clusters in the tidal tails of NGC 3256.

Massive star clusters are formed wherever high gas pressures cause localized star formation efficiencies to exceed 20%–50% (Jog & Solomon 1992; Elmegreen & Efremov 1997; McLaughlin 1999).
Bound star clusters may form whenever the local SFE is above 30% (e.g. Goodwin 1997; Boily & Kroupa 2003 and references therein). Imaging with the Hubble Space Telescope has revealed that young star clusters are formed copiously in the central parts of galaxy mergers, strengthening theories in which giant elliptical galaxies are formed by the merger of spirals (Ashman & Zepf 1992; Whitmore et al. 1993; Miller et al. 1997; Zepf et al. 1999). Young star cluster candidates have also been found in the tidal tails of merging and interacting galaxies (Knierman et al. 2003; Tran et al. 2003; de Grijs et al. 2003; Bastian et al. 2005). Photometric ages suggest that these clusters were formed in the tails, but spectroscopic ages and kinematics are needed to confirm this. Simulations show that the majority of the tails of mergers will probably fall back onto the merger remnant (Hibbard & Mihos 1995). However, the outer parts of the tails become unbound and that material will become part of the intergalactic medium. Therefore, a mechanism exists to inject younger stellar populations in to intracluster regions but kinematics of the young clusters in tidal tails are needed to determine in what instances this occurs.

NGC 3256 is probably one of the best nearby systems for studying the properties of young star clusters in tidal tails. It is a classic merging system, exhibiting a double nucleus (English & Freeman 2003) , a confusion of dust lanes in the central regions, loops and shells surrounding the main body, and two tidal tails that extend up to ∼ 50 kpc in H I(English et al. 2003). Toomre (1977) classified it as intermediate in merger stage between

Electronic address: gtrancho@gemini.edu

FIG. 1.— Position (green square box) of the three star clusters in the Western Tail in NGC 3256.

NGC 4038/39 and NGC 7252. However, it is exceptional in having the highest molecular gas mass, far-infrared luminosity, and X-ray luminosity, and star-formation rate of the mergers in the Toomre sequence (Zepf et al. 1999). Unlike in the Antennae, where they found no cluster candidates in the tidal tails, Knierman et al. (2003) found a significant excess of star cluster candidates in the tidal tails of NGC 3256. The western tail, in particular, has a density of cluster candidates much higher than in the tails of other merger remnants that have been studied. These cluster candidates have V magnitudes between 22 and 26, therefore the brightest can be studied spectroscopically with 8-m class telescopes.

In this paper we present the first results of a large spectroscopic survey of star clusters in galactic mergers/interactions. We focus on three bright star cluster candidates in the western tidal tail of NGC 3256 with GMOS on Gemini South. Other targets in our survey, which will be presented in later works, include the main body of NGC 3256, NGC 4038/39 (the Antennae), NGC 6872, Stephan's Quintet, and M82. The current paper is organized as follows: the observations are described in § 2. We derive the age, mass metallicity, and line-of-sight velocity for each of the clusters in § 3. Finally, we discuss and summarize the results in § 4.

NGC 3256 is located at $\alpha_{\rm J2000} = 10^{\rm h}27^{\rm m}51\overset{\rm s}{.}3$, $\delta_{\rm J2000} = -43°54'14''$ and has a recession velocity relative to the Local Group of $cz_{\rm LG} = +2527 \pm 3$ km s^{-1}, which places it at a distance of 36.1 Mpc for $H_0 = 70$ km s^{-1} Mpc^{-1}. At that distance, adopted throughout the present paper, $1'' = 175$ pc. The corresponding true distance modulus is $(m - M)_0 = 32.79$. The Milky Way foreground extinction is relatively high, $A_V = 0.403$ (Schlegel et al. 1998), whence the apparent visual distance modulus is $V - M_V = 33.19$.

2. OBSERVATIONS AND REDUCTIONS

Imaging and spectroscopy of star cluster in NGC 3256 were obtained with GMOS-S in semesters 2003A and 2004A. The data were obtained as part of two Director's Discretionary Time program GS-2003A-DD-1 and GS-2004A-DD-3. The imaging covers the typical GMOS-S field, which is approximately $5\overset{'}{.}5 \times 5\overset{'}{.}5$. Imaging was obtained through two filters g' and r'. Four GMOS masks were used for the spectroscopy. We used the B600 grating and a slit of $0\overset{''}{.}75$, resulting in a instrumental resolution of 110 km/s at 5100 Å. The spectroscopic observations were obtained as 8 individual exposures with exposure time of 3600 sec each. Spectroscopy of 70 candidates yielded only 50 that were star clusters and only three were located in the tidal tails. In this paper we will focus on these three star clusters. Table 1 lists these 3 star clusters. Column (1) gives the adopted cluster ID, columns (2)-(3) the coordinates, columns (6) and (7) g' and r' magnitudes and errors. The magnitudes have been corrected for Galactic extinction, but not for any internal extinction.

Figure 1 shows the g' image of NGC 3256 (body and western tail) with the observed candidate clusters T1127, T1165 and T1149.

The basic reductions of the data were done using a combination of the Gemini IRAF package and custom reduction techniques. The Gemini IRAF package is an external package built on to the core IRAF. All science images were bias-subtracted and then flat-fielded with Gcal flats which were co-added and normalized. Spectra were extracted and wavelength calibrated with solutions obtained from the arc exposures. The spectra were then combined with cosmic-ray rejection, and flux calibrated using the response function derived from our flux standard. In all cases, we also computed an error spectrum as the square root of the variance of the sum spectrum. To achieve this, the iraf task 'apall' weights each pixel in the sum by an estimated variance based on a spectrum model and detector noise parameters. The error spectrum is then used to facilitate accurate estimation of uncertainties in our analysis.

More details of the reductions will be described in Trancho et al (2007a), hereafter Paper II. Figure 2 displays the flux calibrated spectra of T1227, T1149, T1165 versus the observed wavelength.

3. RESULTS

3.1. *WFPC2 Sizes*

In order to determine the structural parameters of the clusters in this work, we have used archival *F555W-WFPC2/HST* images. The observations are presented in detail in Knierman et al. (2003). Sizes were measured with the *ISHAPE* routine of Larsen (1999), which yielded half-light radii $R_{\rm eff}$. We fitted different profiles (King30, King100, Moffat15 and Moffat25) of multiple sizes. The PSF was generated using *TinyTim* (Krist & Hook 1997) at the exact position of the clusters on the WFPC2 chips. The mean $R_{\rm eff}$ of the above profiles are given in Table 1.

Each of the three clusters is larger than the nominal resolution limit for ISHAPE (FWHM $\sim$ 0.2 pixels; Larsen 2004), which at the assumed distance of NGC 3256 corresponds to a linear distance of 3.2 pc. These clusters are quite extended (average $R_{\rm eff}$ of a Milky-Way GC or YMC is 3−4 pc, whereas the three clusters presented here have effective radii between $\sim 10 - 20$ pc) but still within the range for young clusters (e.g. Maraston et al. 2004; Larsen 2004). These relatively large sizes may reflect weak compression of the GMC at the time of cluster formation (Jog & Solomon 1992, Elmegreen & Efremov 1997). Additionally, since the clusters lie outside the main body of the galaxy their outer envelopes may be not as efficiently stripped by the galactic potential, leaving them rather large (cf. Schweizer 2004).

3.2. *Cluster Properties*

Using the age and metallicity sensitive spectral features, we can determine the properties of the clusters assuming single-burst stellar populations (e.g. Schweizer & Seitzer 1998). However, there are significant differences in resolution, α/Fe-enhancement and range of ages between the model spectra from various groups (e.g. Bruzual & Charlot 2003 [hereafter BC03], Vazdekis 1999 [hereafter Vaz99], Thomas et al. 2004 [hereafter TMB04]). Whereas some models like BC03 have the necessary resolution (3 Å) to match the observations (4.4 Å), others like Vazdekis have twice the resolution (1.8 Å), but they do not extend to very young

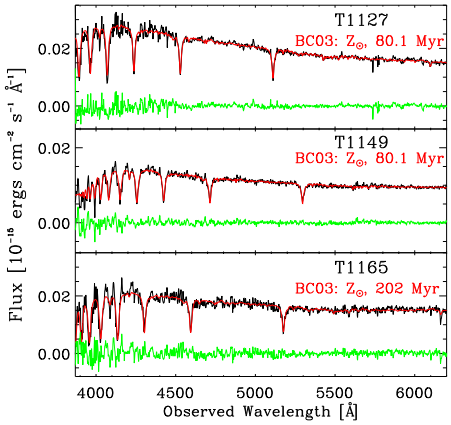

FIG. 2.— Optical spectra of the three young massive clusters T1127, T1165, T1149 (black lines). Overplotted are the model spectra (red lines) for clusters of metallicity $Z_{\odot}$ at different ages by Bruzual & Charlot (2003). We also show the residuals (green lines) in the sense "observed-model".

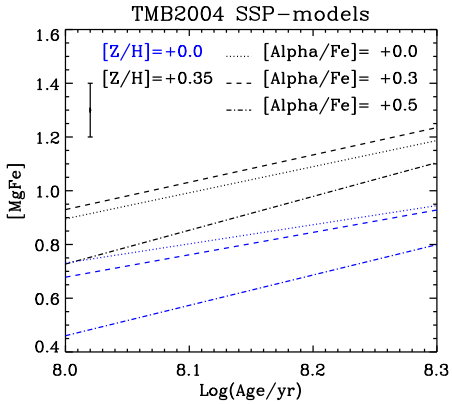

FIG. 3.— Lick indices [MgFe] versus age in model cluster spectra with age TMB04 at different [α/Fe] enrichments. A typical 1σ error bar is shown for reference. Clearly, we cannot differentiate between the various models.

ages. Finally, others like TMB04 have only half the resolution of our observations but these models take into account the effects of changing element abundance ratios on Lick indices, hence give Lick indices not only as a function of age and metallicity, but also as a function of the [α/Fe] ratio.

Therefore, we adopt the following method: First, we use the TMB04 models to confirm that at younger ages the α/Fe-enhancement does not significantly affect age determinations and therefore it can be ignored in the present study. Then we calculate the extinction of our spectra and we use the BC03 models, due to their higher spectral resolution, to measure ages and metallicities calculated from the output spectra using the Penalized Pixel-Fitting method (pPXF; Cappellari & Emsellem (2004)). The pPXF method is based on the Bounded-Variables Least-Squares algorithm. It considers the Line-Of-Sight Velocity Dispersion (LOSVD) of the stars in a cluster as a Gauss-Hermite series and attempts to recover it using a maximum penalized likelihood formalism while working in pixel space. It has the advantage of being robust even when the data have low signal-to-noise ratio (S/N) or when the observed LOSVD is not well sampled. In conclusion, the pPXF method, as realized in an IDL routine, takes in model spectra of different ages/metallicities and weights them in order to create a best fit stellar spectrum.

3.2.1. *[α/Fe] enrichment check*

We used the TMB04 models to check and confirm that at younger ages (less that 500 Myr) the [α/Fe] enrichment does not affect the age determination significantly. Especially when considering our typical error bars (See Figure 3) we cannot differentiate between the various [α/Fe] enrichment models. Figure 3 shows that the [MgFe] vs age diagnostic diagram is relatively free from the age/metallicity degeneracy at younger ages. Iso-[α/Fe] tracks for three different ratios (0.0, 0.3, and 0.5 dex) are plotted.

3.2.2. *Cluster Metallicities, ages, and masses*

In order to estimate the ages of the three tidal tail star clusters, we measured Lick line-strength indices (Faber et al. 1985; González 1993; Trager et al. 1998) and the indices defined by Schweizer & Seitzer (1998) (i.e. HHe, K, H8) from the output spectra using the Penalized Pixel-Fitting method (pPXF) (In Paper II, we will discuss the full details of the fitting method and treatment of errors). The measurements of the indices were carried out with the task INDEX (Cardiel et al. 1998). The errors on the measurements include the influence of photon-statistics and uncertainties in the radial velocities and continuum level.

As a first step in determining the ages and metallicities we plot the [MgFe] ratio vs. Hγ of the BC03 models for four different metallicities and all available ages in Fig. 4. The metallicity index [MgFe] is defined through [MgFe] =[Mgb $\times$ (0.72 $\times$ Fe5270 + 0.28 $\times$ Fe5335)]$^{1/2}$ (Thomas et al. 2003) , where Mgb, Fe5270, and Fe5335 are Lick indices expressed in Angstroms. We then over plot the observed clusters and their 1σ error bars.

This diagram yields cluster metallicities of $2/5Z_{\odot}$ – $2.5Z_{\odot}$ ($\sim$2 sigma range) for T1127, T1149, and T1165. We also plot W3, a massive young cluster in the merger remnant NGC 7252, for comparison. W3 has an age of 500 Myr and a metallicity of 1.0 $Z_{\odot}$ (Schweizer & Seitzer 1998).

However the absorption-line indices shown in Fig. 4 are just one of various possible combinations of line indices which we have measurements for. In order to fully exploit the observations we compare all seven indices shown in Table 2 to the BC03 models weighted by their respective errors in a least χ^2 sense. The values of the indices are given in Table 2. In order to test how robust the ages and metallicities derived are we perform the following test. We add random errors to each measured line index, where the added errors are selected from a normal distribution with a standard deviation of the observed error. We then find the best fitting age and metallicity, and repeat this process 5000 times for each cluster. Finally, we fit a Gaussian to the (logarithmic) age distribution to get the peak and standard deviation. The results for the age distribution are shown in Fig. 5. If the 3σ errors are used the results stay the same but the standard deviation increases by about a factor 3.

As an additional check on the derived ages we also fit the full spectral shape of the observed clusters to the BC03 models including extinction. We apply the standard galactic extinction law (with A_V ranging from 0 to 10 mag) to the BC03 models in steps of $\Delta A_V = 0.1$ and

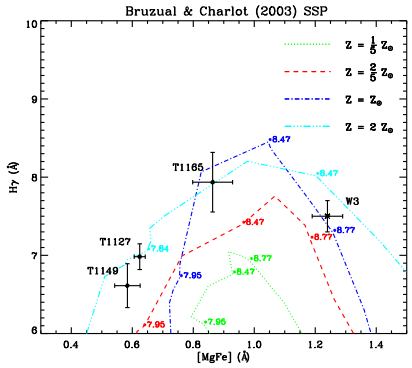

FIG. 4.— Determination of ages and metallicities of the clusters. Hγ vs. [MgFe] from the BC03 SSP models for four different metallicities are shown with the measures and errors (1σ) form the cluster spectra are shown.

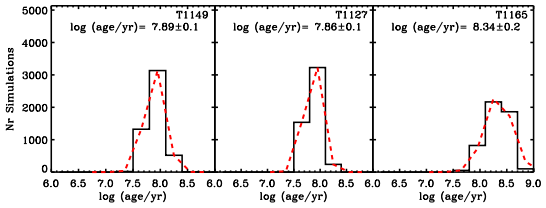

FIG. 5.— Histogram of the ages derived by simulating the effect of the errors on the age fitting routine. See the text for the details of the simulations. Note that T1127 and T1149 appear to be coeval while T1165 appears to be significantly ($\sim$ 2.3 times) older than the other two.

compare each model (24 age and 100 extinction steps) to the observed cluster spectra in a χ^2 sense. The fits were carried out between 4000 and 5500 Å. In all three cases presented here, the ages determined for the clusters through spectral indices were in excellent agreement with the results of fitting the spectral shape, giving us further confidence in the accuracy of the derived ages. The derived extinctions are shown in Table 1.

The metallicities are also derived from the indices fitting test. We take the above simulations and take the mean metallicity weighted by the number of simulations which gave each metallicity as the best fit. Doing this we find metallicities of 1.3 ± 0.7, 1.8 ± 0.6, and 1.4 ± 0.6 solar for T1127, T1149, and T1165 respectively.

Once the ages are known we can derive the photometric masses of the star clusters by comparing their g'-band magnitude to that of the BC03 SSP models of the appropriate age. The derived masses are given in Table 2, where we have assumed a Chabrier (2003) initial mass function (IMF) for the clusters. The derived masses would be approximately 1.5 times higher if one assumes a Salpeter (1955)-type IMF. All three clusters appear to be quite massive, being very close to the average mass of globular clusters in the Galaxy. As mentioned in § 3.1, the fact that the clusters lie outside the main body of the galaxy suggests that they will not be significantly affected by the tidal field of the galaxy. Thus, these clusters are not expected to loose a large amount of their mass due to tidal effects, so their mass loss will be dominated by stellar evolution and two-body relaxation.

3.3. *Cluster Velocities*

Table 3 gives the heliocentric radial velocities $cz_{\rm hel}$ measured for the three star clusters. These velocities represent averages of velocities measured by two different methods. First, we determined a mean velocity from 6−7 absorption lines (Hβ through H8, Ca K, and Na D) measured individually in each cluster spectrum. And second, we also determined a mean velocity for each cluster via cross-correlation. As a template we used the spectra of three radial-velocity standards observed with the same resolution (HD 100953, HD 126248 and HD 133955). Results from the two methods agreed to within the combined errors, and the velocities given in Table 3 represent the straight average of the two mean velocities measured for each cluster.

Table 3 also gives the projected distance $r_{\rm p}$ of each cluster from the galaxy center and the cluster velocity Δv relative to the nucleus of NGC 3256. This relative line-of-sight (LOS) velocity was computed from

$$\Delta v = (cz_{\rm hel} - cz_{\rm hel,sys})/(1 + z_{\rm hel,sys}),$$

where the denominator is a relativistic correction and the systemic velocity of NGC 3256 is $cz_{\rm hel,sys} = 2818 \pm 3$ km s^{-1}. The latter velocity is the straight average of four high-quality values published in the literature: 2820 ± 15 (Feast & Robertson 1978), 2817 ± 10 (Lípari et al. 2000), and 2820 ± 11 km s^{-1} (English & Freeman 2003) from Hα-velocity mapping, and 2814 ± 11 km s^{-1} from the H I velocity profile (Koribalski et al. 2004).

The values of Δv for the three clusters lie in the range $-154 \lesssim \Delta v \lesssim -67$ km s^{-1}, indicating that all three clusters are physically associated with NGC 3256 and, specifically, with its western (W) tail. Neutral hydrogen observations with the Australia Telescope Compact Array show that this tail as a whole appears blue-shifted relative to the center of the galaxy (English et al. 2003, esp. Fig. 8). The optical Δv of Cluster T1127 agrees with the local H I velocity in the tail to within the combined errors. However clusters T1149 and T1165 both feature optical LOS velocities $\sim$80 km s^{-1} lower than the local H I velocity. This may simply reflect the coarse resolution and heavy smoothing of the H I velocity map as the mean diameter of the synthesized beam is 23″. *If* these young clusters are associated with the H I gas, then their relative LOS velocities Δv indicate that the approach velocity of the W tail is nearly twice as large (about -150 km s^{-1}) as previously inferred from the H I. An alternative possibility, however, is that the clusters have already decoupled kinematically from the local gas.

The main reason why clusters eventually decouple from the surrounding gas is that the gas experiences, and reacts to, pressure forces in addition to gravity, while clusters orbit subject only to gravity. (Of course, gravity fields fluctuate during a merger, but that alone would not separate gas from stars, since both feel the same gravity.)

The most distant of the three clusters, T1149, moves with a relative LOS velocity of $\Delta v = -154 \pm 16$ km s^{-1}. Assuming for a moment that its transverse motion is of similar magnitude, this $\sim$80 Myr old cluster may have moved $\sim$11 kpc in the plane of the sky since its birth, or nearly half of its present-day projected distance from the center. This allows the possibility that this cluster, and perhaps also the other two tail clusters, may have formed significantly closer to the center of the galactic system, presumably as part of the tail-ejection process during the first close encounter of the two participating disks.

If so, the cluster is likely to follow a highly eccentric orbit within the merger remnant.

However, we emphasize that in the absence of any detailed spatial and kinematic model for NGC 3256, the unknown geometry of the W tail prevents us from drawing any firm conclusion about the likely true spatial motions of the three clusters. Depending on whether the clusters lie behind or in front of the sky plane through the center of NGC 3256, their velocities Δv may contain a component directed toward or away from the galaxy's center.

4. SUMMARY AND DISCUSSION

We have studied the ages, metallicities, and [α/Fe] ratios of three tidal tail cluster in NGC 3256 based on the Lick index system. The main results are:

1. T1149 and T1127 appear to be coeval, although T1165 is 2.3 times older than those two ($\sim$200 Myr vs. 80 Myr). T1165, T1127 and T1149 ages are consistent with being formed in the tail. Therefore it appears that cluster formation can proceed over extended periods of time in tidal tails (i.e. tidal structures may not be coeval). This is consistent with the findings of Bastian et al. (2005) for the star clusters in the tidal tails of NGC 6872.

2. All clusters (T1127, T1149 and T1165) are consistent with solar metallicity to within 1σ.

3. All three clusters appear to be quite massive, with masses greater than 10^5 $M_\odot$, similar to the average mass of Galactic globular clusters. Due to the position of the clusters outside the main body of NGC 3256, the clusters are not expected to loose a significant amount of their mass due to interactions with the tidal field of the galaxy.

4. We find also that these clusters are quite extended,with half-light radii of $\sim 10-20$ pc but still within the range for young clusters (e.g. Maraston et al. 2004; Larsen 2004). These large sizes may reflect weak compression at the time of formation and/or the weak influence of the tidal field of the galaxy.

5. All three clusters have velocities consistent with the general trend of the velocity structure of the tail. However, only T1127 (the closest to the galaxy center) has a velocity consistent with the local HI velocity, while T1149 and T1165 have velocities $\sim$ 80 km/s lower than the HI. This could be due to T1149 and T1165 being kinematically decoupled from the surrounding gas or possibly to the lower spatial resolution of the HI data.

All this is in agreement with the dynamical time since the beginning of the merger, which is $\sim$ 500 Myr (English et al. 2003). Finally we conclude that if the loosely bound tail material gets stripped during future interactions in the group, these three clusters may well become part of the intra-group medium.

G.T. would like to thank to Matt Mountain and Phil Puxley for the tremendous support throughout this project.

Based on observations obtained at the Gemini Observatory, which is operated by the Association of Universities for Research in Astronomy, Inc., under a cooperative agreement with the NSF on behalf of the Gemini partnership: the National Science Foundation (United States), the Particle Physics and Astronomy Research Council (United Kingdom), the National Research Council (Canada), CONICYT (Chile), the Australian Research Council (Australia), CNPq (Brazil) and CONICET (Argentina)

REFERENCES

Aguerri, J. A. L., Gerhard, O. E., Arnaboldi, M., Napolitano, N. R., Castro-Rodriguez, N., & Freeman, K. C. 2005, AJ, 129, 2585
Ashman, K.M. & Zepf, S.E. 1992, ApJ, 384, 50
Bassino, L. P., Cellone, S. A., Forte, J. C., & Dirsch, B. 2003, A&A, 399, 489
Bastian, N., Hempel, M., Kissler-Patig, M., Homeier, N. L., & Trancho, G. 2005, A&A, 435, 65
Boily, C. & Kroupa, P. 2003, MNRAS, 338, 665
Bruzual, G. & Charlot, S. 2003, MNRAS, 344, 1000
Cardiel, N., Gorgas, J., Cenarro, J., Gonzalez, J.J. 1998, A&AS, 127, 597
Chabrier, G. 2003, PASP, 115, 763
Jog, C.J., & Solomon, P.M. 1992, ApJ, 387, 152
Cappellari, M., & Emsellem, E. 2004, PASP, 116, 138
de Grijs, R., Lee, J. T., Clemencia Mora Herrera, M., Fritze-v. Alvensleben, U., & Anders, P. 2003, New Astronomy, 8, 155
Elmegreen, B. G., & Efremov, Y. N. 1997, ApJ, 480, 235
English, J., & Freeman, K. C. 2003, AJ, 125, 1124
English, J., Norris, R. P., Freeman, K. C., & Booth, R. S. 2003, AJ, 125, 1134
Faber, S.M., Friel, E.D., Burstein, D., Gaskell, C.M. 1985, ApJS, 57, 711
Ferguson, H. C., Tanvir, N. R., & von Hippel, T. 1998, Nature, 391, 461
Feast, M. W., & Robertson, B. S. C. 1978, MNRAS, 185, 31
Goodwin, S.P. 1997, MNRAS, 284, 785
González, J.J. 1993, Ph.D. thesis, Univ. of California, Santa Cruz
Hibbard, J. E. & Mihos, C.J. 1995, AJ, 110, 140
Jordán, A., West, M. J., Côté, P., & Marzke, R. O. 2003, AJ, 125, 1642
Kissler-Patig, M., Grillmair, C. J., Meylan, G., Brodie, J. P., Minniti, D., & Goudfrooij, P. 1999, AJ, 117, 1206
Knierman, K.A., Gallagher, S.C., Charlton, J.C. et al. 2003, AJ, 126, 1227
Koribalski, B.S. et al. 2004, AJ, 128, 16
Krick, J. E., Bernstein, R. A., & Pimbblet, K. A. 2005, ArXiv Astrophysics e-prints, arXiv:astro-ph/0509609
Krist, J. & Hook, R. 1997, "The TinyTim Users Guide", STScI
Larsen, S.S. 1999, A&AS, 139, 393
Larsen S.S. 2004, A&A, 416, 537
Lípari, S., Díaz, R., Taniguchi, Y., Terlevich, R, Dottori, H., & Carranza, G. 2000, AJ, 120, 645
Maraston, C., Bastian, N., Saglia, R.P., Kissler-Patig, M., Schweizer, F., Goudfrooij, P. 2004, A&A, 416, 467
McLaughlin, D. E. 1999, AJ, 117, 2398
Mihos, J. C., Harding, P., Feldmeier, J., & Morrison, H. 2005, ApJ, 631, L41
Miller, B., Whitmore, B.C., Schweizer, F., Fall, S.M. 1997, AJ, 114, 2381
Murante, G., et al. 2004, ApJ, 607, L83
Salpeter, E.E. 1955, ApJ, 121, 161
Schlegel, D. J., Finkbeiner, D. P., & Davis, M. 1998, ApJ, 500, 525

TABLE 1
PROPERTIES OF THE TIDAL-TAIL CLUSTERS. (THE MAGNITUDES HAVE BEEN ONLY CORRECTED FOR GALACTIC EXTINCTION BUT NOT FOR INTERNAL EXTINCTION).

ID	RA (J2000)	Dec (J2000)	g' (mag)	r' (mag)	A_V (mag)	Mass (10^5 $M_\odot$)	R_{eff}[a] (pc)
T1127	10:27:38.50	-43:54:19.9	22.2±0.1	22.0±0.1	0.3	1.5±0.2	10.9±0.5
T1149	10:27:35.88	-43:52:51.1	22.2±0.1	22.1±0.1	0.0	1.5±0.2	10.2±1.2
T1165	10:27:37.88	-43:53:45.1	22.4±0.1	22.2±0.1	0.5	2.8±0.2	20.7±2.7

[a] Mean R_{eff} using the King30, King100, Moffat15 and Moffat25 profiles with ISHAPE routine

TABLE 2
INDICES

ID	HHe[a] (Å)	K[a] (Å)	$H8$[a] (Å)	$H\gamma$[b] (Å)	$Mgb5177$[b] (Å)	$Fe5270$[b] (Å)	$Fe5335$[b] (Å)	log age (years)
T1127	7.84±0.72	0.73±0.42	6.96±0.74	6.61±0.56	0.49±0.23	0.58±0.29	0.95±0.44	7.8±0.1
T1149	7.82±0.61	0.53±0.37	6.99±0.65	6.98±0.32	0.53±0.15	0.63±0.20	0.96±0.29	7.8±0.1
T1165	9.55±1.41	0.85±0.89	8.59±1.56	7.93±0.76	0.77±0.36	0.87±0.45	1.20±0.64	8.3±0.2

[a] Indices definition by Schweizer & Seitzer (1998).[b] Lick indices.

TABLE 3
CLUSTER POSITIONS AND RADIAL VELOCITIES

Cluster	r_p ($''$)	r_p[a] (kpc)	cz_{hel} (km s^{-1})	σ_{cz} (km s^{-1})	Δv[b] (km s^{-1})
T1127	140	24.5	2750	19	−67
T1149	189	33.1	2663	16	−154
T1165	150	26.3	2685	16	−132

[a] For $D = 36.1$ Mpc ($H_0 = 70$ km s^{-1} Mpc^{-1}).[b] Line-of-sight velocity relative to nucleus, $\Delta v = (cz_{hel} - 2818)/1.00940$ (see text).

Schweizer, F. 2004 in ASP Conf. Ser. 322, "The Formation and Evolution of Massive Star Clusters", eds. H.J.G.L.M. Lamers, L.J. Smith, A. Nota, p. 111
Schweizer, F., & Seitzer, P. 1998, AJ, 116, 2206
Trager, S.C., Worthey, G., Faber, S.M., Burstein, D., Gonzalez, J.J. 1998, ApJS, 116, 1
Tran, H. D., et al. 2003, ApJ, 585, 750
Thomas, D., Maraston, C., & Bender, R. 2003, MNRAS, 343, 279
Thomas, D., Maraston, C., & Korn, A. 2004, MNRAS, 351, L19
Toomre, A. 1977, in Evolution of Galaxies and Stellar Populations, ed. B. Tinsley & R. Larson (New Haven: Yale Univ. Press), 401
Vazdekis, A. 1999, ApJ, 513, 224
West, M. J., Cote, P., Jones, C., Forman, W., & Marzke, R. O. 1995, ApJ, 453, L77
Whitmore, B.C., Schweizer, F., Leitherer, C., Borne, K., Robert, C. 1993, AJ, 106, 1354
Yahagi, H. & Bekki, K. 2005, MNRAS, in press (astro-ph/0509744)
Zepf, S. E., Ashman, K. M., English, J., Freeman, K. C., & Sharples, R. M. 1999, AJ, 118, 752

This figure "fig1.jpg" is available in "jpg" format from:

http://arXiv.org/ps/astro-ph/0612136